Final Technical Report (UMD AMAV)

The UMD AMAV Horizon tailsitter drone was created for the 2022-2023 VFS DBVF competition

1. Executive Summary

Objective: Under the VFS Design-Build-Vertical-Flight Competition guidelines, the University of Maryland Autonomous Micro Air Vehicle (AMAV) team's objective is to design and fabricate an unmanned aerial vehicle capable of completing a flight performance and an autonomy course. A rendering of the UMD AMAV's tailsitter design Horizon is shown above.

Purpose of Design: The design of the Horizon vehicle is to balance hover and cruise performance with autonomous flight capabilities while remaining under strict competition guidelines such as weight limit, payload requirement, dimensions, and overall design quality. Safety, reliability, and component and flight testing processes also inform and validate the overall design process.

Planned Approach: The UMD AMAV team's plan for the VFS DBVF Competition involved a multistep process to create a successful design. We began by creating a detailed schedule that reflects our design, manufacturing, and testing processes (Section 2). The design started by outlining the mission requirements to create a design plan (Section 3.1). We narrowed down the priorities for our design based on the competition scoring criteria, budget constraints, and manufacturing feasibility (Section 3.2). From the breakdown of the design priorities, we investigated a number of configurations to determine the best fit for this competition (Section 3.3). After populating a decision matrix, we selected our final design configuration to be a *tailsitter configuration* (Section 3.4). While the overall goal of the design is to be successful in

the competition, we emphasized uniqueness and incorporated the latest manufacturing technologies (Section 4). To move forward from this preliminary design to the final design (Section 5), 3D drawings were developed to allow traceability of the design process (Section 6). Our manufacturing process included facilities and resources available at the University of Maryland, as well as vendors providing specialized services (Section 7). At the end of the final design stage, we tested every component of our vehicle to ensure its reliability (Section 8 and 9). The completed tests validate the overall performance of the vehicle. Additional tests and full mock mission tests are ongoing and will continue up until the final presentation (Section 9) and flight exhibition, as appropriate.

2. Management Summary

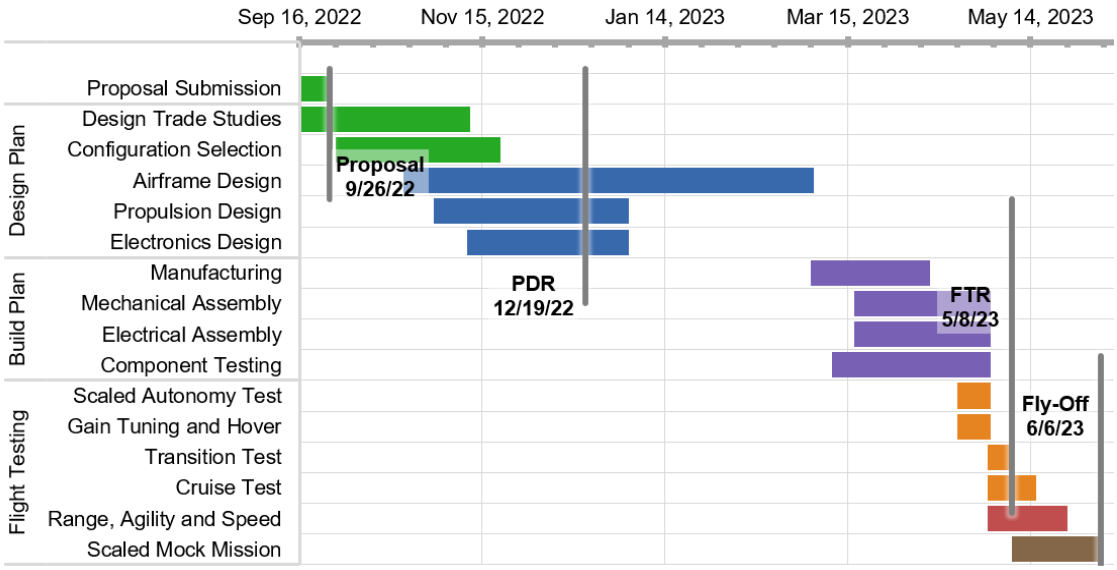

Schedule: A Gantt chart showing the complete Horizon build and flight test timeline is provided below. Ordering electronics is a long-lead-time process and, therefore, we pre-ordered critical electronics such as the flight controller and FPV system. Cruise testing is a high-risk process and so the flight testing will use a gradual flight-envelope-expansion testing process.

Team Organization: The UMD Autonomous Micro Air Vehicle (AMAV) team is composed of undergraduate, graduate, and Ph.D. students from various majors, including aerospace engineering, mechanical engineering, computer science, and robotics. The team is guided by advisor Professor Derek Paley and co-advisor Joshua Gaus. The team's affiliated team members are listed below (* denotes participants in the flyover event). This year's entry in the VFS DBVF is the UMD AMAV Horizon.

Name	Email	Class Standing	Role
Prof. Derek A. Paley	dpaley@umd.edu	Faculty	Advisor
Joshua Gaus *	jgaus@umd.edu	Project Engineer	Co-Advisor
Animesh Shastry *	animeshs@umd.edu	PhD AE	Team Lead
Dilhara Jayasundara	dilharaj@umd.edu	PhD AE	Aerodynamics Lead
Qingwen Wei *	qwei@umd.edu	BS AE	Design Lead & Pilot

Alex Wang *	awang130@umd.edu	BS ME	Design & Pilot
Dhruv Srinivasan	dhruvs@umd.edu	BS ME	Design & Manufacturing
Madeline Brode	madelinebrode@gmail.com	BS AE	Design & Manufacturing
Ron Berlin *	rberlin8@terpmail.umd.edu	BS AE	Design & Manufacturing
Justin Cheng	jcheng17@umd.edu	MEng. Robotics	Design & Manufacturing
Sabrina Zaleski	szaleski@terpmail.umd.edu	BS ME	Design & Manufacturing
Leonello Castro Cillis	leonello.castro.cillis@gmail.com	BS AE	Design & Manufacturing
Shubham Takbhate *	stakbhat@umd.edu	MEng. Robotics	Design & Manufacturing

3. Design Trade Studies

3.1. Mission Requirements

The Horizon vehicle must be able to successfully complete the following two courses to earn points as dictated by the rubric on the VFS Request for Proposals.

Flight Performance Course: This course tests the vehicle's agility and endurance by having the vehicle complete as many laps of a predetermined course as it can in under ten minutes. Prior to takeoff, a 2-lb SoftGrip weight is attached to the vehicle with an option for heavier weights. The vehicle must perform a full VTOL landing at the end of each lap and then perform a VTOL take-off to begin the next lap. The course is scored on three parameters: time for the first three laps, number of laps completed, and payload weight, each of which is scored out of 50.

Autonomy Course: The vehicle must maneuver autonomously through the course using pre-set GPS coordinates. This includes both VTOL take-off and landing. A successful completion of the course yields 150 points.

3.2. Design Drivers

Endurance and Maneuverability: For the competition, our primary goal is to fly as fast as possible to maximize the number of laps within the allotted 10 minutes flight time. Approximately 66% of the overall fly-off points comes from the endurance and maneuverability of the design. Hence, we sought a design with a greater motor thrust-to-weight ratio and higher control authority to increase our ability to accelerate quickly and minimize turning radius.

Weight/Dimensions: For the aircraft design, one of our goals was to make the best use of the provided dimensional constraints. The competition presents us with a 10ft maximum span and a maximum weight of 20-lb including the 2-lb payload. Since 33% of the overall points come from our payload fraction, part of our team's design process involves leaving ample room for additional payload weight. The payload fraction is also affected by the aircraft weight and thus an oversized aircraft will have a negative impact on payload fraction score.

Cost and Reliability: We factored in the cost of components into our overall decision process. We selected lower-cost alternatives without sacrificing reliability wherever possible.

Design Complexity: It is important that the proposed aircraft design is not overly complex, since it may impact manufacturing time, cost, and reliability. Furthermore, unnecessary complexity may have a negative impact on controllability. During the design process, we valued configurations that are not too complex, which might hinder manufacturing or ease of piloting.

3.3. Configurations Considered

The configurations considered focus on maximizing speed and efficiency between waypoints. The nature of the mission's timed component led the team to favor configurations with a fast cruise speed; however, the ability to transition between hover and forward flight is an important caveat to this decision-making. The team also focused on designs in which autonomous navigation, including forward-flight and hover transition control actions, are relatively easy to implement. The following configurations were considered.

Configuration	Description
	**Quadrotor** - Most common drone configuration; four rotors - Control angles determined by varying RPM of motors - Forward flight achieved by pitching vehicle forward
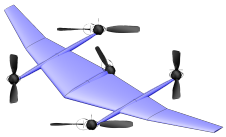	**Quadplane** - Configuration has four rotors with fixed wing/aircraft fuselage - Forward flight conducted by pusher propeller - Pitch, roll determined by varying rotor RPM or aircraft control surfaces
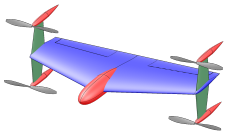	**Quadrotor Tailsitter** - Configuration that starts vertically, then tilts the entire fuselage forward to transition into forward flight - Transition achieved by pitching vehicle forward by 90°
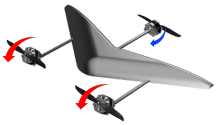	**Tiltrotor** - Configuration with either two or three tilting rotors - Control angles determined by tilting rotors - Forward flight achieved by tilting rotor along vehicle's longitudinal axis

3.4. Selection Process and Final Design

3.4.1. Analysis of Alternative Configurations

Prior to selection, an internal review of the configuration is conducted for configuration finalization. Factor weightings and ultimate decisions are cataloged in a decision matrix. The quadplane and tiltrotor configuration have some similarities that may overlap in design, so the quadplane model is assumed to be a four-rotor model with a pusher/tractor propeller, whereas the tiltrotor is a tricopter configuration. We use the Analytical Hierarchy Process (AHP) method to obtain weights for each of the parameters. The resulting Pugh Matrix is given in Table 1.

The two most important parameters that influence the team's decision are safety and reliability, followed by maneuverability and endurance. A high thrust-to-weight ratio provides greater maneuverability of the vehicle. In the case of both the tailsitter and tiltrotor, the aforementioned parameter also allows the vehicle to achieve cruise speed faster. Payload fraction is also an important parameter. A lower frame weight allows for a higher payload capacity. In addition to the aforementioned parameters, we also consider cost and design complexity. While there is no restriction on the amount spent, the team values designs whose parts may be

manufactured in-house through methods such as additive printing. Design complexity embodies ease of assembly, ease of disassembly, and pilot control.

3.4.2. Selection and Customization of Final Design

Based on the decision matrix, we selected the quadrotor tailsitter configuration for this year's design. The timed nature of the flight performance course strongly incentivizes a fast cruise speed between waypoints with fewer actuators such as motors or servos. The quadplane, tiltrotor, and quadrotor tailsitter all perform well in this category, but the quadrotor tailsitter has the least weight; this design maximizes the payload fraction.

Table 1. Pugh Matrix for Configuration Selection. The various configurations were compared against the Quadrotor baseline and scored from +3 to -3 denoting the degree of fulfillment of each design goal.

Design Driver	**Score Weight**	**Quadrotor**	**Quadplane**	**Quad-Tailsitter**	**Tiltrotor**
Endurance	*1.4*	0	+3	+3	+3
Maneuverability	*1.5*	0	-2	-1	-2
Payload Fraction	*0.5*	0	-2	-1	-2
Cost	*0.2*	0	-1	-2	-2
Reliability	*1.7*	0	+1	+1	+1
Design Complexity	*0.3*	0	-2	-2	-3
Forward Flight Performance	*0.5*	0	+3	+2	+3
Safety	*2.2*	0	0	0	-1
Final Score		**0.0**	**2.6**	**3.9**	**-0.1**

4. Technical Innovations

4.1. Design Innovations

Pylons to act as winglets: The pylons that connect the propellers to the wing are designed to act as winglets that not only reduce the loss of lift by blocking the tip vortices but also generate forward thrust (Coiro et al., 2008), resulting in a lower drag. A symmetric airfoil shape is used to ensure the lift force generated by both the upper and lower winglets is tilted forward so that they generate a thrust component in the forward direction to counteract the drag. The wingtip vortex creates a spanwise flow component near the tip of the wing. This causes the winglets to have an effective angle of attack with the incoming flow. Using CFD simulations, we estimate 27% gain in aircraft lift-to-drag ratio with the winglet design compared to an alternative flat-plate design.

Vortex generators: By delaying local flow separation and aerodynamic stalling, vortex generators improve the effectiveness of wings and control surfaces at and beyond stall angles. They lower the stall speed of the aircraft making it more controllable at lower speeds. However, vortex generators also increase drag and thus require increased power required to fly at higher speeds. Vortex generators may be added to the wing if any stall issues arise during flight testing.

4.2. Manufacturing/Technology Innovations

3D Printing: Due to the fast-paced nature of the competition timeline, we are taking advantage of 3D printing technology. We can choose between different types of plastic, polymer, and

carbon-based filaments to create customized parts. We can also take advantage of 3D printing to create parts with geometries that would be much more complicated or not possible to machine.

4.3. Mission Model

Modeling the aerodynamics of the wing post stall is beyond the scope of this report. Hence, we will describe the model used for power prediction in hover and cruise flight only.

Assumptions and uncertainties: Standard rotorcraft flight assumptions include 30% electrical-to-mechanical energy conversion efficiency loss, 30% propeller efficiency loss, flight at ISA+15^{0}C conditions (air density ϱ=1.224 kg/m^3), and canceling of rotor in-plane forces and moments due to symmetric placement of rotors.

Sources of Inputs: The other main input into the mission power estimation model is the aerodynamic force model. The aerodynamic lift and drag coefficients are obtained from VLM and CFD analysis of the wings; see Section 4.3.

Detailed Model Description: The power estimation model is based on momentum theory. Hover power is calculated using the following expression

$$P_{\text{hover}} = \frac{1}{\eta_{\text{conv}}} \frac{1}{\eta_{\text{prop}}} \frac{T^{1.5}}{\sqrt{2\rho A}} + P_{\text{avionics}}$$

where η_{conv} is the conversion efficiency, η_{prop} is the propeller/rotor efficiency, A is the total rotor disk area, and T is the thrust, which is equal to the aircraft weight. In cruise, the propellers operate in climb and the total power is obtained using the following expression:

$$P_{\text{cruise}} = \frac{1}{\eta_{\text{conv}}} \frac{1}{\eta_{\text{prop}}} T \left(\frac{v_{\text{cruise}}}{2} + \sqrt{\frac{T}{2\rho A} + \frac{v_{\text{cruise}}^2}{4}} \right) + P_{\text{avionics}}$$

where v_{cruise} is the aircraft's cruise speed and thrust T is equal to the total drag force, which can be calculated from the lift and drag model of Section 4.3.

5. Design Definition

4.1. Overall Vehicle Design

The UMD AMAV Horizon shown in Figure 2 is a hybrid VTOL tailsitter aircraft consisting of four motors organized in a quad configuration, also known as a Quadrotor Monoplane Tailsitter. It is tailless to reduce weight; elevons present on the wing helps in control.

5.1. Vehicle sub-system design

5.1.1. Airframe Design

Airfoil Selection: Our initial choice for wing airfoil was the PW51 airfoil due to its extremely low moment coefficient and thin profile, which would have led to lower drag and higher top speed. However, with PW51, structural issues arose as fitting a 1" (0.0254 m) thick spar would lead to a very high lower bound on the wing chord. Hence, we selected the MH60 airfoil for the wing as it is thicker than PW51 and so better able to accommodate the wing spar while reducing the lower bound on the chord and without compromising on the moment coefficient.

Wing Sizing: The design of the wing balances safety, handling, structure and aerodynamic efficiency properties. Preliminary selection of propulsion and avionics components and

simplifying assumptions on airframe and payload weight led to an estimate of gross takeoff weight (GTOW) of 13.2 lbs (6 kg). A stall speed of 31 mph (14 m/s) was selected based on pilot's experience, which also leads to safer flight at lower cruise speeds. Assuming the aircraft's maximum lift coefficient of 0.8, the desired wing area is 0.62 m^2. A tailless aircraft has swept tapered wings and so the tip chord is chosen at the lower bound value of 15" (0.38 m). For selecting sweep angle, a high value would result in better handling and stability but can also lead to a discontinuous wing spar thereby compromising structure. Hence, to accommodate a continuous wing spar, a 25° leading edge sweep angle is selected, which results in a root-chord of 26" (0.66 m) and wing span of 48" (1.22 m) in order to achieve the desired 0.6 m^2 wing area. The aspect ratio of the wing is 2.3, which is lower than standard, but is an acceptable compromise that balances safety, handling, structure and aerodynamic efficiency properties. Figure 1 shows the dimensional design of the wing.

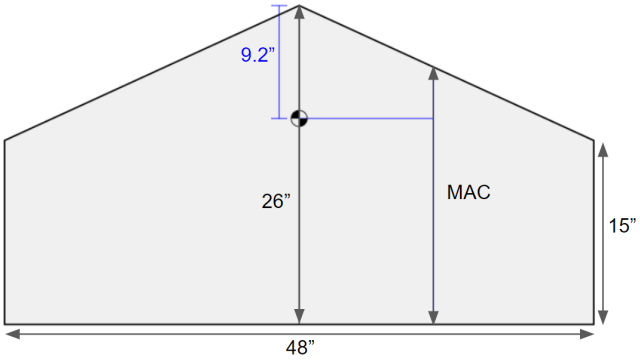

Fig. 1. Horizon wing dimensional design

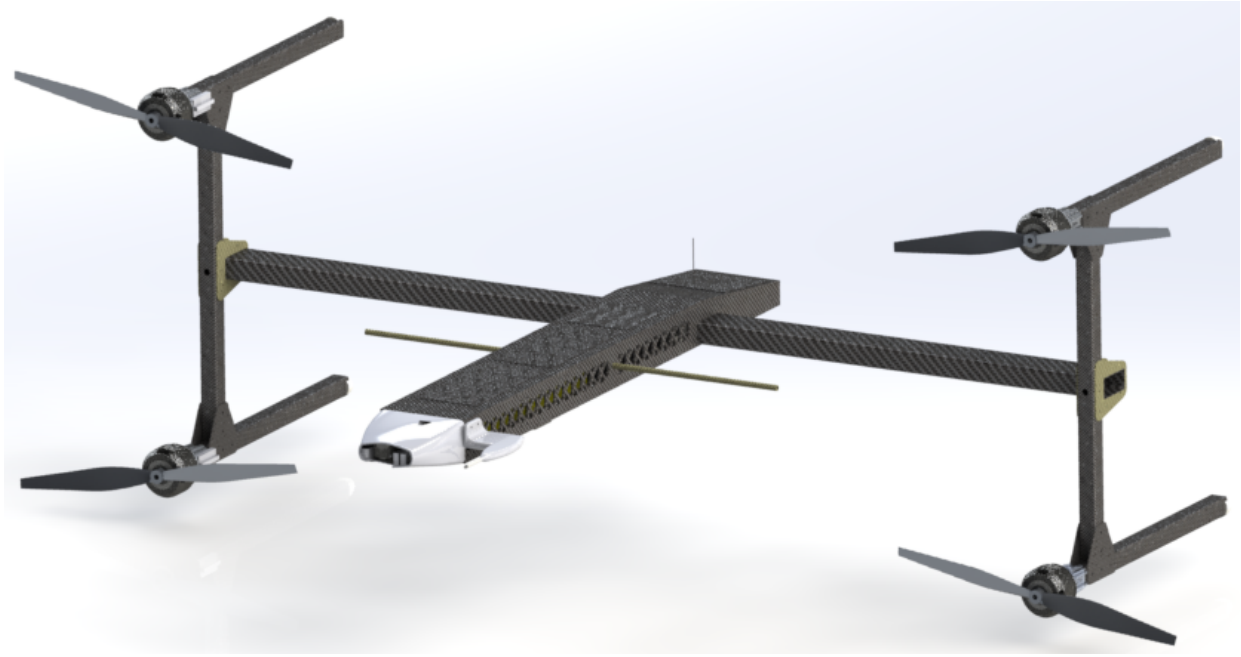

Fig. 2. Overall Design of UMD Horizon. The main wing is hidden to show the airframe.

5.1.2. Propulsion System Selection

Motor and Propellers: Selection of the motor and propeller is determined by the desired compromise between efficient hover and high-speed cruise flight. We constrain the selection to fixed pitch, variable-RPM systems as there are a variety of options to select from and because the mechanical simplicity is beneficial for safety and reliability. The off-the-shelf availability of propellers also constrains the selection. We considered 12x12, 15x10, and 18x5.5 propellers from

APC. A lower-diameter, higher-pitch propeller leads to higher maximum speed of the aircraft, whereas a higher-diameter, lower-pitch propeller is desirable for efficient hover flight. The 12x12 propeller will lead to the highest maximum speed, but it stalls in the hover/static condition. Between 15x10 and 18x5.5 propellers, the 18x5.5 is better for hover efficiency, but its lower pitch leads to lower maximum cruise speed. Hence, a 15x10 propeller strikes a balance between high speed cruise and hover performance. To get a desired maximum thrust-to-weight ratio of 3 in hover, the motor needs to have the specification of maximum continuous power greater than 1.1kW. Next, we identified that in order to achieve a maximum speed of 40m/s for the aircraft, the motor kV needs to be in the range of 400-500kV. Both 420kV and 490kV motors from the U7 series of T-motor fit our needs. The 490kV motor gives higher maximum RPM and thereby higher cruise speed, but it also will run considerably hotter, which is detrimental to the magnets. Hence, we chose 420kV for safer flight and longer operational life.

Batteries: We selected a dual 6S (22.2V) 4500mAh battery setup, since it provides a 10-minute hover time and 10-minute cruise time at 35m/s (see Section 4.3).

5.1.3. Electronics/Avionics

Horizon has Pixhawk Cube Orange as the onboard flight controller. External sensors connected to it include Here3 GPS, Matek Airspeed sensor, and current sensor. Additionally, a DJI O3 Air Unit on the aircraft enables high-resolution digital video transmission for FPV flight.

5.1.4. Autonomous Flight and Transition Control

We use QGroundControl as our ground control station (GCS) software to configure and upload autonomous waypoint missions to the Pixhawk through MAVLink via radio telemetry. During the transition of the aircraft from hover to cruise and vice versa, the pilot input is disabled and the attitude and throttle of the aircraft is controlled by the flight controller. In case of any errors, transition is aborted and the pilot takes control of the aircraft.

5.2. Aircraft Structural Analysis

The aircraft structure is primarily composed of hollow carbon fiber tubes that form the spar of the main wing and the winglets. In hover, the structure experiences the maximum stress since the weight of the aircraft is concentrated at the motor mounting points whereas in cruise, the weight is distributed along the main wing's spar. Hence, structural analysis in hover was conducted and two spar-structure configurations were compared. Configuration 1 was designed by using two 0.75" square cross-section tubes separated by 5" distance as the main wing's spar, whereas configuration 2 consists of a single 2"x1" rectangular cross-section tube as the main wing spar. As for the winglet spars, both configurations utilize 0.75" square cross-section tubes. Figure 3 shows the Factor of Safety plot for both spar configurations. Additionally, harmonic analysis was performed to determine the top resonant frequencies of the structure. Table 2 shows the overall results, from which we conclude that for a similar weight, configuration 2 has a better factor of safety along with higher resonant frequency modes. Essentially, Configuration 2 is both stronger and stiffer than Configuration 1. Figure 4 shows an exaggerated displacement plot for the lowest two resonant frequencies of both configurations.

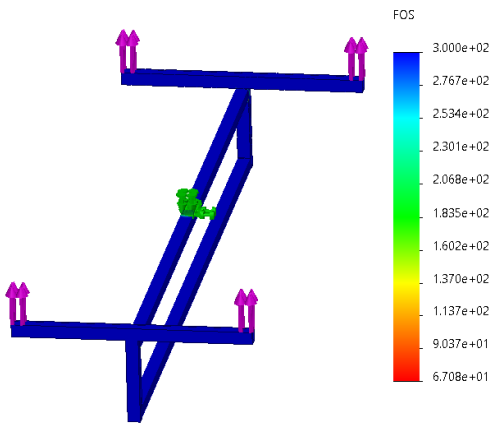

(a) Spar Config 1: Structure composed of 0.75" square carbon fiber tubes only

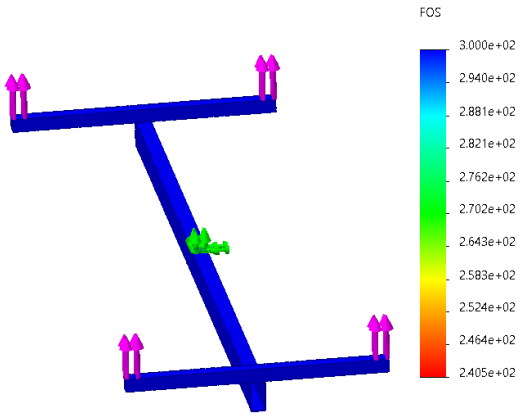

(b) Spar Config 2: Structure composed of 2"x1" rectangular and 0.75" square carbon fiber tubes

Fig. 3. Factor of Safety results from Finite Element Analysis of competing spar configurations

Table 2. Comparison of FEA results of competing structure configurations

	Spar Configuration 1	**Spar Configuration 2**
Weight	2.08 lb	1.98 lb
Factor of Safety	67	240
Res. Freq. Mode 1	32 Hz	49 Hz
Res. Freq. Mode 2	53 Hz	95 Hz

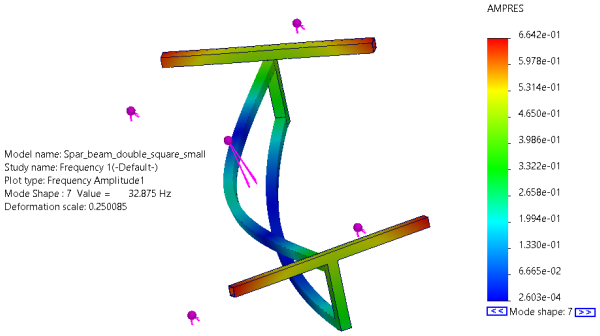

(a) Spar Config 1; Res. Freq. Mode 1

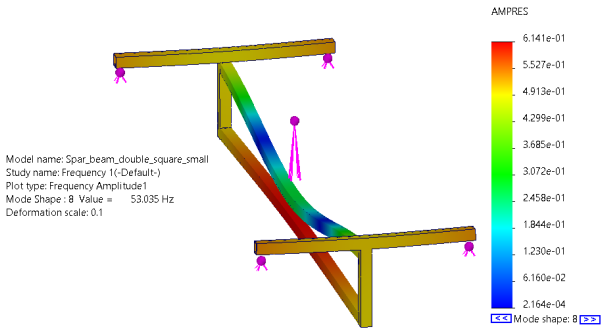

(b) Spar Config 1; Res. Freq. Mode 2

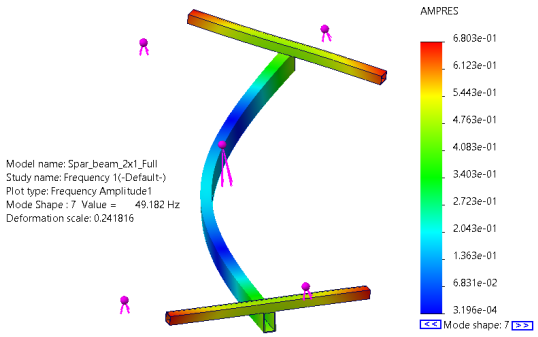

(c) Spar Config 2; Res. Freq. Mode 1

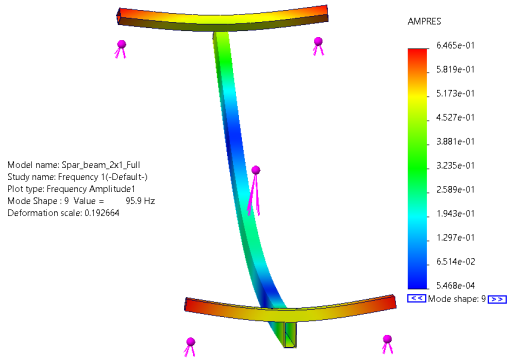

(d) Spar Config 2; Res. Freq. Mode 2

Fig. 4. Competing structure configurations' displacement at lowest two resonant frequency modes

5.3. Aircraft Performance Analysis

Predicted Mission Performance: The power estimation model described in Section 3.3 is used to calculate the total power required by the vehicle at various cruise speeds as shown in Figure 5. Conservative estimates are made for the efficiency parameters along with 75% depth of battery discharge. At hover, the endurance obtained is 10 min. The best endurance is obtained at the minimum power requirement. The best endurance speed is 16 m/s and the maximum endurance is 31.2 min. The best range occurs at the minimum drag condition, which is the point where the power-to-speed ratio is minimum. The best range speed is 21 m/s and the maximum range is 34.3 km (21.3 miles). The maximum speed for the vehicle is around 40 m/s, due to the thrust produced by each propeller decreasing to 3.7N at 7500 RPM, the maximum motor speed.

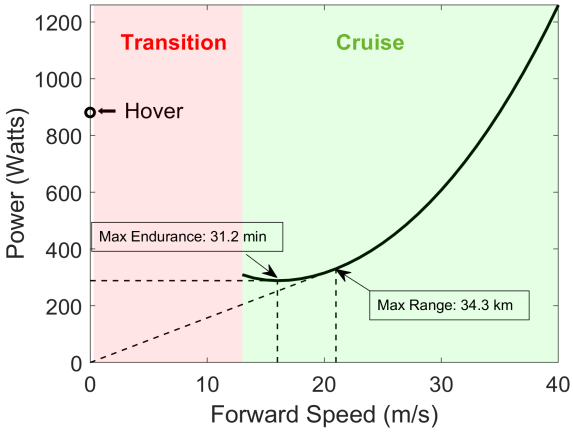

Fig. 5. Aircraft power vs. forward speed

Weight and Balance: The total weight of the aircraft is 13.2 lbs (6 kg). The top three components with the highest weight are flight battery, motors, and payload. The aircraft components are arranged in a manner that brings the aircraft's CG close to the desired location of 9.2" (0.23 m) from the wing tip. Figure 6 shows the aircraft's weight composition in grams and percentage.

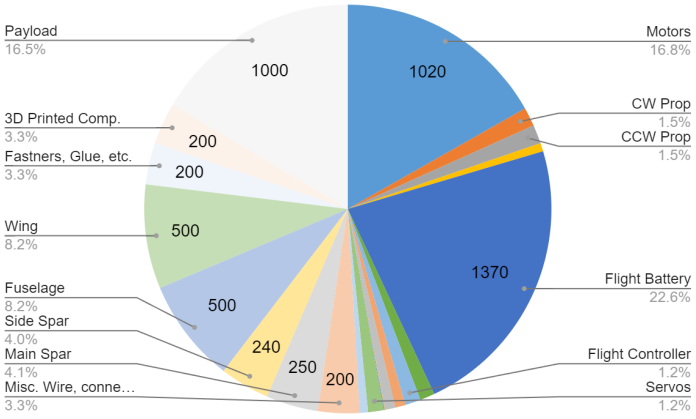

Fig. 6. Pie chart showing the weight composition in grams

Table 2. Lift and drag attributes at various AoA and preset angles

Wing Preset (°)	Wing AoA (°)	CL	CD	L/D
0	0	0.10	0.025	4.0
0	6	0.54	0.047	11.3
0	12	0.95	0.105	9.0
2	2	0.23	0.027	8.5
6	6	0.50	0.042	11.9

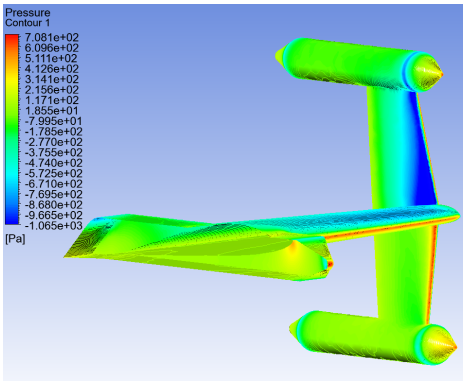

Fig. 7. Pressure contours from CFD

Aircraft Lift and Drag Estimation: We use the Vortex Lattice Method (VLM) method provided by OpenVSP as well as the Ansys Fluent computational fluid dynamics (CFD) package to estimate the lift and drag characteristics of the aircraft. Results from Ansys are shown in Figure 5 and summarized in Table 2. VLM prediction for lift-to-drag ratio (L/D) is shown in Figure 8. The

MH60 airfoil's max efficiency is at 6° angle of attack (AoA) to the incoming flow. However, mission safety prioritizes low stall speed and, hence, a larger wing area. To trim the aircraft, no extra preset angle is needed, so that the aircraft sees a 0° AoA at the maximum cruise speed of 40 m/s. The aircraft has a L/D of 4.0 at 0° tilt and it goes up to 11.3 at a 6° tilt angle. From these

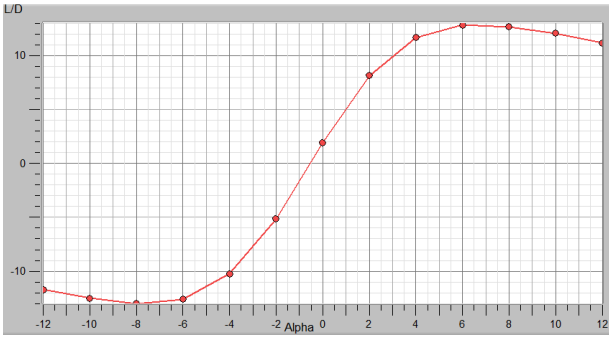

Fig. 8. L/D vs. AoA as predicted by VLM

data, the following lift and drag coefficient model was developed.

$$C_D = 0.024 + 0.173C_L^2, \quad C_L = \frac{2W}{\rho v_{\text{cruise}}^2 S} = \frac{158.2}{v_{\text{cruise}}^2}, \quad \text{for } v_{\text{cruise}} > v_{\text{stall}} = 14\text{m/s}$$

Aircraft Stability: The desired CG location is chosen at 9.2 inch (0.23 m) from the tip, which is at the 20% location of the mean aerodynamic chord (MAC). This choice yields a 5% static stability margin. To balance the resulting pitch moment, a spanwise twist of -3° is needed. Due to twist, the outer regions of the span will experience less lift than the inner regions; hence, to trim the aircraft at a cruise speed of 35 m/s, a 2° preset was also added. Using XFLR5, the longitudinal and lateral eigenvalues of the aircraft were calculated and are shown in Figure 9.

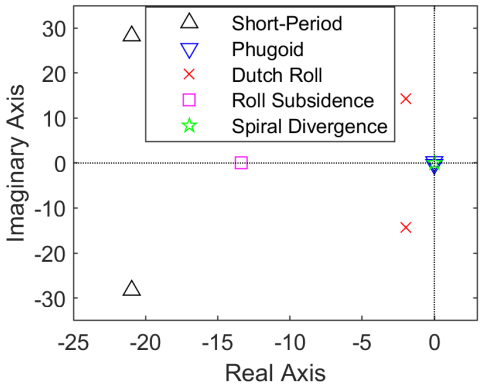

Fig. 9. Longitudinal and Lateral Modes

6. Drawing Package

Fig. 10. Structural arrangement drawing of the aircraft showing the internal structure

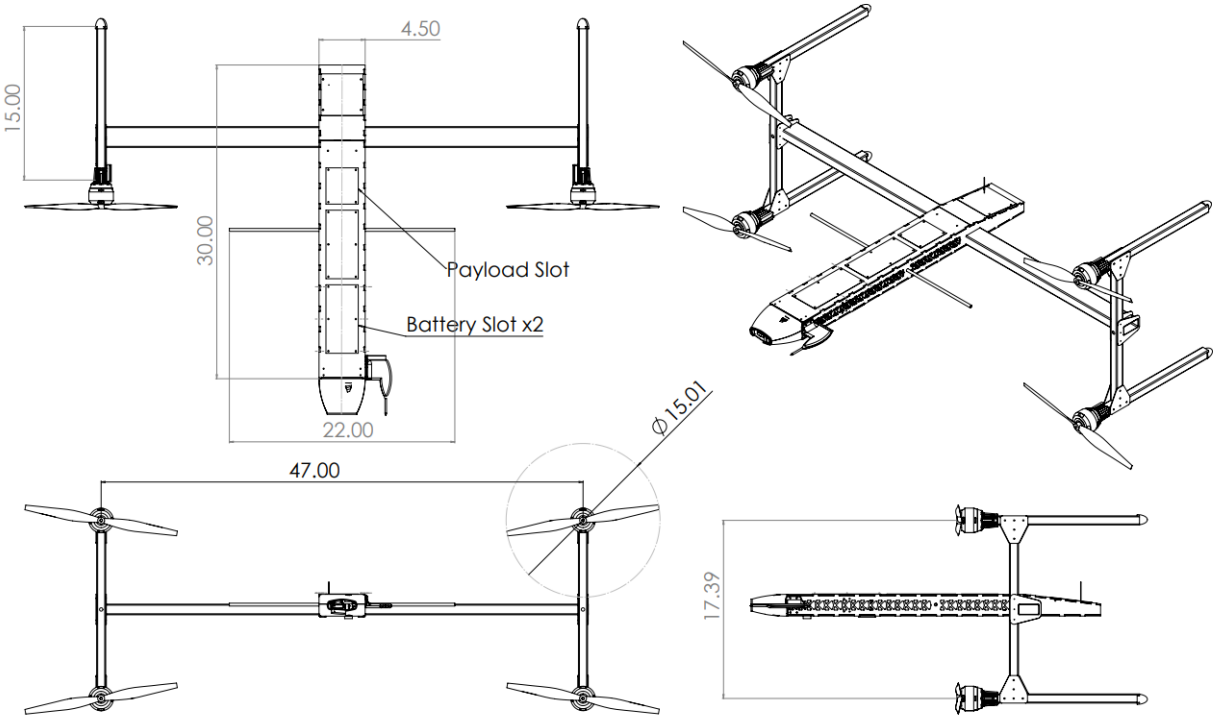

Fig. 11. Three View and Isometric Drawing of the Aircraft. Dimensions are in inches. Wings are hidden to show the internal structure and components.

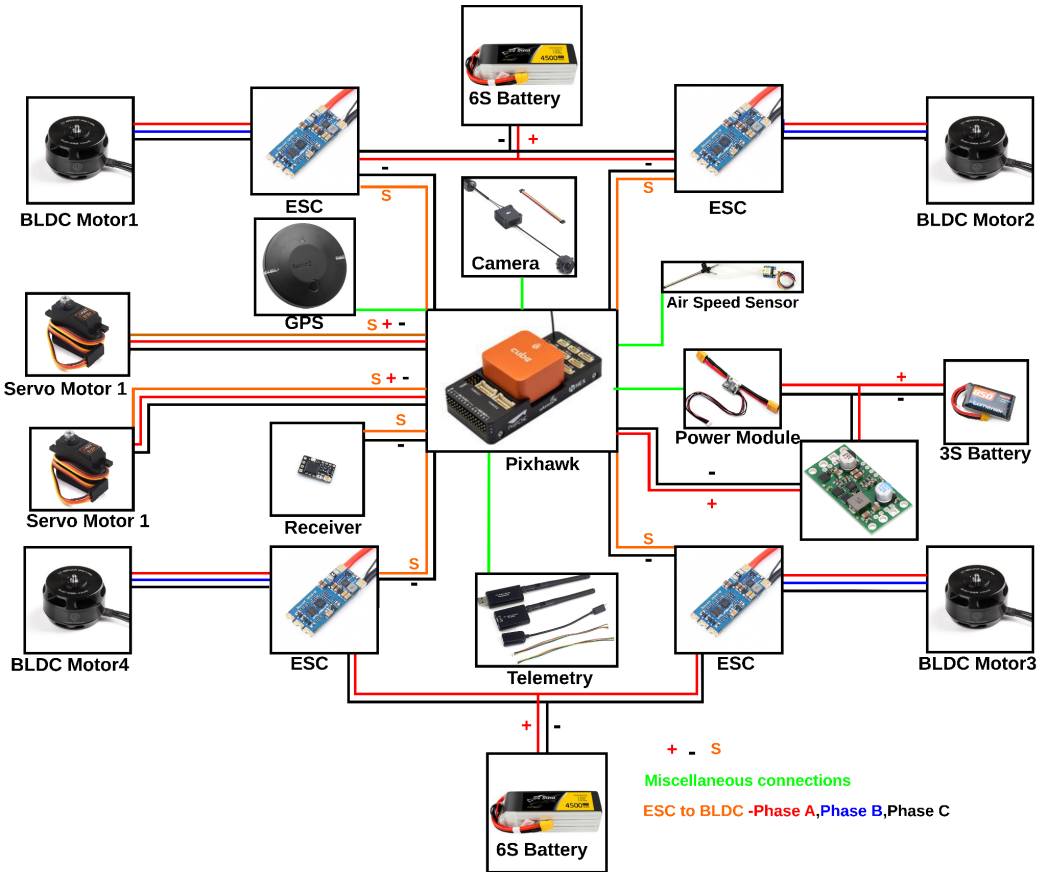

Fig. 12. Propulsion and Avionics Systems wiring diagram

7. Fabrication Methods

7.1. Manufacturing processes investigated, discussed, and compared

Based on the team's prior experience in participating in past VFS AMAV student competitions, we chose appropriate materials and fabrication methods to quickly manufacture and assemble a completely custom aircraft in the timeline given by the competition. Factors such as weight, strength, cost, assembling/printing time, and specialized tool requirements guided the downselection of the manufacturing process.

7.2. Considered Methods/Materials

CNC Machining: For our main body and structure, we considered Dragon Plate, carbon fiber and wood sandwich, and normal carbon fiber. Dragon plate provides a lightweight option, but it loses strength from using a wood core and has a higher chance of delamination. Due to the complexity of the carbon fiber plate components, we investigated automated machining methods such as CNC and waterjet as the primary means of manufacturing.

3D Printing: As nearly the entire aircraft is custom made, for mounting and other hardware parts, we used 3D printing. The main materials considered are PLA, ABS, and Onyx. PLA has a tensile strength of 37 MPa and 1.3 g/cm^3 density. ABS is the next choice as it has a higher 110 MPa tensile strength and a lower 1 g/cm^3 density. However, ABS is harder to print as it requires higher printing temperatures and has a higher chance of warping. We also used Onyx with Carbon Fiber reinforcement, which has a tensile strength much higher than PLA and ABS, while being a similar weight. The downside of this material is that it is much more expensive, meaning that we used it only for very specific applications where the high strength is necessary, such as the motor mounts.

Hot Wire CNC Cutting: We used EPP foam for the skeleton of our wing. Due to its durability and strength with a low density of .03 g/cm^3, it is the ideal material to sustain the wing loads while remaining lightweight. We used hot wire CNC cutting as it is ideal when manufacturing foam structures.

7.3. Final Manufacturing Process

Custom Component Manufacturing: Standard carbon-fiber plate is selected as the primary material for the aircraft due to its low weight, high strength, low cost, and manufacturability. The skeleton of our aircraft consists of a carbon fiber frame and EPP foam for the wing. The primary 3D printing material is CF reinforced onyx; it is used on most of the custom structural/mounting components. Certain aircraft components required epoxy bonding where steel/aluminum fasteners were not feasible.

Assembly: Most of the components on the aircraft are screw-mounted and reinforced with Loctite to diminish the effects of vibration-induced loosening of the screws. Electronics and mechanical assembly has been carefully executed and tested thoroughly.

8. Test Plan

Fig. 13. The UMD Fearless Flight Facility

Hover flight tests in quadrotor configuration are performed indoors in the UMD Brin Family Aerial Robotics lab and outdoors at the UMD Fearless Flight Facility (F3), due to the 15-mile no-fly zone established by the FAA around Washington D.C.. Compared to the the competition location, F3 (Figure 13) is relatively small: 100x300x50 feet, which results in scaled -down tests compared to the competition. The cruise flight tests will be conducted at the University of Maryland UAS Test Site to ensure safe operation in an environment where flight tests are routinely completed.

8.1. Flight Worthiness Test

Test objectives: Determine if the drone is in proper mechanical and electrical condition.

Test setup: To examine how well the parts such as motors, propellers, flight controllers are fixed, the drone is started on the ground and a little thrust is applied to see if the drone tilts to the intended direction and to hear the sound of it to determine whether the motors operate as intended. To ensure good electrical performance, transmission voltage losses must be within 2% and component's temperatures must be in a safe range during and after flights.

8.2. Hover Endurance Test

Test objectives: Determine how long the drone can hover in place and establish its reliability for the duration of the battery life.

Test setup: The test is conducted inside the netted area of Fearless Flight Facility (F3).

8.3. Cruise Endurance Test

Test objectives: Determine how long the drone can cruise with forward flight.

Test setup: The test is conducted in F3 and performed autonomously, in order to maintain the consistency of the drone's speed. The drone circles around to make a similar situation of the test. Also the vehicle's extra payload carrying capacity beyond the minimum 2 lb is tested.

8.4. Agility and Speed Test

Test objectives: Determine the maneuverability and cornering ability of the drone.

Test setup: In this test, the pilot manually flies the drone in acrobatic mode (attitude rate control) and pushes the drone to the limit of its performance.

8.5. Autonomous Flight Test

Test Objectives: Determine how accurate the autonomous capabilities of the drone are by programming numerous waypoints in the testing facility. Additionally, evaluate landing accuracy by characterizing the range of position error using the same autonomous mission and same predetermined landing point to see exactly where the drone lands each time.

Test Setup: The GPS capabilities of the drone is tested by flying in position-hold mode, which is the mainstay prerequisite before testing. Initially, simple waypoint missions like take off, fly 10 feet, and land are tested. The complexity of these missions is increased to establish reliability, eventually leading up to a mock mission. Furthermore, to test landing accuracy, a simple autonomous mission is created with one landing point and is executed multiple times. After each mission, the landing position of the drone is marked on the ground.

9. Flight Test Results

Flight Worthiness Test [Complete]:

The initial flight worthiness test was completed in the Brin Family Robotics Lab with the propellers removed from the drone. Using Mission Planner, the motors were tested at 15% throttle to ensure functionality and the correct direction of spinning. Once it was determined that the motors were all working as intended, as well as that all of the arming checks were met and the drone would arm when desired, we tested using the controller inputs. The motors correctly responded to each controller input, and we confirmed by listening for the faster spinning of two sets of motors for each input. Finally, we tested to ensure that the drone could be disarmed from the controller. Once all of these checks were completed, the team deemed the drone sufficient for the hover endurance test.

Hover Endurance Test [Complete]:

The initial vertical flight test was completed in the Fearless Flight Facility, with the intention to demonstrate that vertical flight in quadrotor mode was possible, and that the drone could reliably take off and land from a fixed position. The drone was successfully able to arm, lift off, and land reliably, as well as respond correctly to all of the desired controller inputs. After the initial hover testing was aborted due to an anomaly, the team is now working forwards to implementing several changes to improve flight performance including tuning the flight controller parameters.

Cruise Endurance Test: Not yet completed. See schedule for expected date of completion.

Agility and Speed Test: Not yet completed. See schedule for expected date of completion.

Autonomous Flight Test: Not yet completed. See schedule for expected date of completion.

10. Conclusion

The technical report describes the entire procedure by which we designed and are in the process of finalizing the building and testing operations of our aircraft for the 2022-2023 VFS DBVF competition. We met or exceeded the design requirements and are planning to complete the bonus task as well. The aircraft will be thoroughly tested before the competition. Ongoing and future work seeks to further enhance the aircraft's performance, decrease its weight, and expand its autonomous capabilities.

10. References

Coiro, D.P., Nicolosi, F., Scherillo, F. and Maisto, U., 2008. Improving hang-glider maneuverability using multiple winglets: a numerical and experimental investigation. *Journal of Aircraft*, *45*(3), pp.981-989.